POLITECNICO DI TORINO
Repository ISTITUZIONALE

Temperature monitoring of tumor hyperthermal treatments with optical fibers: comparison of distributed and quasi-distributed techniques

(Article begins on next page)

01 September 2025

Temperature monitoring of tumor hyperthermal treatments with optical fibers: comparison of distributed and quasi-distributed techniques

Alessandra Beccaria, Aurora Bellone, Alessandro Mirigaldi, Valentina Serafini,
Massimo Olivero, Alberto Vallan, Guido Perrone

Politecnico di Torino, Dept. of Electronics and Telecommunications
C.so Duca degli Abruzzi 24; I-10029 Torino; Italy
email: firstname.lastname@polito.it

Corresponding author: Guido Perrone; guido.perrone@polito.it

Abstract

Optical fiber based sensors capable of measuring temperature distribution over a given length are particularly attractive in the biomedical field, especially in the case of real-time monitoring of minimally invasive hyperthermal treatments of tumors, such as laser ablation, given their intrinsic multiplexing along a single fiber span and the unique properties of optical fibers in terms of flexibility, size and electromagnetic compatibility. The paper compares two sensing approaches: one is based on an array of Bragg gratings inscribed in the core of a single-mode fiber, the other detects Rayleigh backscattering from an unmodified single-mode fiber using coherent optical frequency domain reflectometry. Following an introduction, which describes the most distinctive features of the two approaches, the paper presents three comparative experiments, each devised to highlight a peculiar aspect of the sensors. In the first experiment the sensors are exposed to various constant temperature distributions to evaluate the uniformity of the readings along the fiber length. In the second experiments, a known temperature profile is generated through an *ad-hoc* setup to evaluate the actual capability of the two approaches to reconstruct the temperature distribution. Finally, in the third experiment the two sensors are employed in a simulated tumor laser ablation procedure to measure the temperature distribution in the irradiated area. Both sensors provide results whose error, mainly due to cross sensitivity between temperature and strain, is acceptable for the considered biomedical application.

Keywords

Distributed sensing
Fiber Bragg grating sensors

Optical frequency domain reflectometry

Tumor laser ablation

Temperature measurements

1 Introduction

Fiber Optic Sensors (FOSs) are finding increasing applications in engineering, fundamental science and medicine for their unique combination of versatility, high sensitivity, immunity to electromagnetic interference, possibility to operate in harsh environment, and remote interrogation using the same fiber both for sensing and for data transmission [1, 2]. Particularly remarkable is the growth in the biomedical field since, besides for the previously listed characteristics, FOSs have a minimal invasive impact due to the small diameter and flexibility of fibers, and are intrinsically free from electrocution [3, 4]. Moreover, they are fully compatible with Magnetic Resonance Imaging (MRI), one of the most powerful imaging techniques, which can therefore be used for their optimal positioning.

One of the most striking feature of FOSs is the distributed sensing capability, which is traditionally obtained by multiplexing several point sensors along the same fiber, often Fiber Bragg Grating (FBG) sensors [5, 6]. However, since in practice the distance among the sensing points can vary from centimeters to several meters, these configurations should be more precisely called "quasi-distributed sensing system". Indeed, more recently, new dedicated equipment for assembling truly distributed sensing systems in which the spatial resolution can be as fine as some tens of micrometers have appeared on the market, drawing an enormous interest, as demonstrated by current and projected sales [7, 8] and the number of scientific papers on this topic in the last years (see for example, [9–11], to name a few).

Targeting specifically medical applications, distributed or quasi-distributed sensing systems find one of their most innovative and relevant use cases in measuring temperature distribution profiles for the real-time monitoring of minimally invasive ablation treatments of tumors [6, 12–14]. These are relatively new surgical procedures in which a localized hyperthermia well above cytotoxic levels is induced in the tumor mass using electromagnetic waves. Depending on the frequency band used, the technique is called Radio-Frequency Ablation (RFA), Micro-Wave Ablation (MWA) and Laser Ablation (LA). LA is the most recently introduced ablation technique and therefore still the least investigated but shows excellent potentialities, especially in terms of overall costs versus the achievable benefits and patient discomfort [15]. In order to optimize the ablation treatment, a reconstruction of the induced temperature distribution map is required [16]. To do so, not only FOSs are optimal but, in the specific case of LA, they are also the only choice a part from imaging techniques – MRI, Ultrasound (US) or Computed Tomography (CT) – because of the absence of artifacts induced by the interaction between the laser beam and the sensor, as happens using, for instance, thermocouples [12]. Distributed fiber optic sensing techniques are mainly based on Raman [17], Brillouin [18], and Rayleigh [19, 20] scattering. Clearly, each of these approaches has its own strong and weak points, but all of them deal with very low signals and therefore require complex – thus expensive – instruments

and quite long measurement time, resulting in severe limitations in dynamical applications. Nevertheless, all these techniques have been successfully employed in a wide range of strain or temperature sensing applications. For biomedical temperature measurements, and especially for LA monitoring, particularly useful is exploiting the Rayleigh scattering through the Optical Frequency Domain Reflectometry (OFDR) because it allows achieving a temperature resolution down to 0.1 °C with sub-millimeter spatial resolution [20]. Rayleigh backscattering is induced by random fluctuations in the fiber refractive index profile along the fiber. The scattered amplitude is therefore random as well, but it is a static function, characteristic of an unperturbed and at constant temperature fiber; hence, when an external stimulus is applied (e.g., a change in temperature, or a local strain), the pattern of these random fluctuations changes, modifying the reflection spectrum.

On the other hand, quasi-distributed sensing system can be easily realized by multiplexing several FBGs. FBGs are fabricated by inducing a variation in the core refractive index resulting in a periodical structure that generates a reflectivity peak at a wavelength, called the Bragg wavelength (λ_B). A change in temperature causes a variation both in the refractive index and in the lengths producing a shift in λ_B. This way, the temperature sensing is based on a wavelength shift and not on a modification in the received amplitude, making this approach robust also in noisy environments. However, as the Bragg wavelength shifts are typically small (about 10 pm/°C), quite complex interrogation techniques have to be used if a temperature resolution down to 0.1 °C is required [21]. Moreover, the spatial resolution is limited by the length of the periodic structure forming the FBG, which is in the order of millimeters. This non negligible size introduces also temperature measurement errors when the sensor is used in presence of large thermal gradients, as it occurs during laser ablation procedures [22–24]. In quasi-distributed sensing applications up to 40-50 FBG sensors – each with a different λ_B – can be cascade multiplexed along a single fiber, the number being limited by the interrogator spectral bandwidth and by the necessity of guaranteeing that the spectra do not overlap taking into account the temperature induced shifts. On the plus side, multi-channel interrogators are available and high measurement speeds in the order of kilohertz are possible.

In this work we analyze the two different approaches to measure a temperature profile – a actual distributed system based on OFDR and a quasi-distributed one based on multiplexed FBGs – during laser ablation procedures, comparing the two both in ad hoc experiments and in simulated ablation procedures.

The paper is organized as follows. In Sec. 2 an overview of the working principles of the FBGs and of Rayleigh scattering based distributed sensing systems is provided; then in Sec. 3 the experimental setup is explained in detail, covering the measurement setup, the FBG fabrication, and the comparative experiments. Finally, in Sec. 4 the conclusions are drawn.

2 Instruments and methods

Measuring a temperature profile with multiplexed FBGs requires inscribing a set of FBGs with different Bragg wavelength in the core of an optical fiber. In early times, this was done by

exposing the fiber to an intense UV-laser; today, a femtosecond laser is preferred. The first fiber Bragg grating inscription using a high energy femtosecond laser source was reported in 2003 [25]. This inscription process is based on the absorption phenomenon induced by focusing the femtosecond laser beam into the fiber core, which causes an highly localized deposit of energy into an electron plasma that is formed within the focal volume. This energy is then adsorbed by the underlying lattice which undergoes a permanent and localized material modification (e.g., localized melting, creation of defects, material compaction, micro-void formation, nano-grating etc.), the type of modification being determined by the intensity of the laser pulse and the irradiation conditions. With respect to the FBGs induced by UV sources, the femtosecond laser induced FBGs can be inscribed in any optical waveguide and are more thermally stable, which makes them of particular interest for sensing in harsh environments [26].

The inscription process can be done either point by point or using a phase mask. In the former method the laser pulses are individually focused into the fibre core through a high numerical aperture microscope objective while the fiber translates; this approach is more critical from the point of view of mechanical stability requirements, but it allows fabricating structures with any periodicity and therefore is particularly suited for fabricating multiplexed gratings for quasi-distributed sensing without having to splice separately written FBGs (which, besides for requiring extra fabrication steps, it would also severely limit the spatial resolution and the uniformity of the separation between the sensing points). On the other hand, the phase mask approach allows reducing the alignment tolerance requirement, but as it requires different masks for inscribing different FBGs, it not suited for the realization of chains of gratings. Therefore, the FBGs used in the experiments presented in this paper have been written using the point by point technique with a laser micro-machining workstation from Workshop of Photonics, which is based on a femtosecond laser by Light Conversion. In particular, considering the application of tumor laser ablation, the gratings have been inscribed in the core of a Double Cladding Fiber (DCF) [6]; the core diameter is about $9\,\mu m$, similar to that of standard single-mode fibers used for telecommunication applications. During the inscription process, both reflection and transmission spectra have been monitored using a supercontinuum source and optical spectrum analyzer coupled through a circulator and a switch, as sketched in Fig. 1.

The inscription process induces a modification in the refractive index of the order of 10^{-4}. Performing a periodic point by point inscription, the resulting fibre core is described by the equation:

$$
\begin{cases}
n_{\rm c} = n_0 + \Delta n & 0 < x \le \Lambda\,({\rm DC}) \\[2mm]
n_{\rm c} = n_0 & \Lambda\,({\rm DC}) < x < \Lambda
\end{cases}
\tag{1}
$$

where $n_{\rm c}$ is the core refractive index after the writing process, n_0 the core original refractive index, Δn the change in the refractive index induced by the femto inscription, DC the duty cycle and Λ the period of the grating. As well known, the Bragg wavelength $\lambda_{\rm B}$ is given by [27]:

$$
\lambda_{\rm B} = 2 n_{\rm eff}\,\Lambda
\tag{2}
$$

where $n_{\rm eff}$ is the effective refractive index of the fiber, which in turns depends on Δn and DC. Environment modifications such as temperature and strain, affect the period and the local
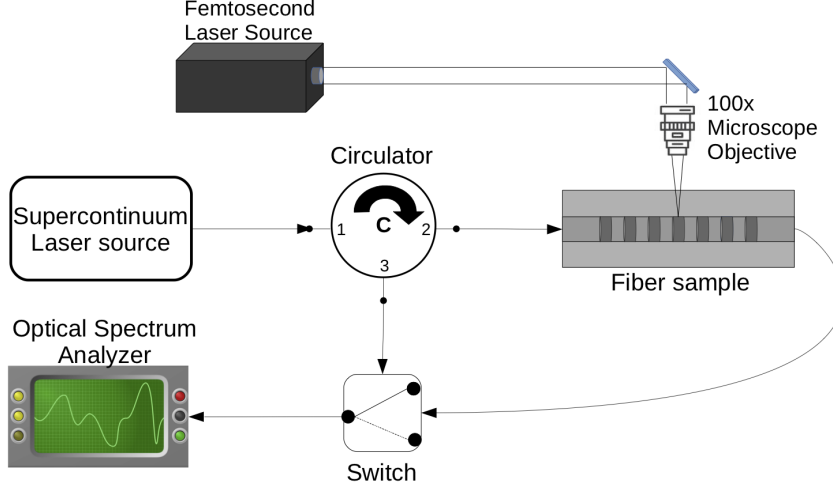
Figure 1: Schematic illustration of the optical setup employed for the real time monitoring of the FBGs inscription procedure.

refractive index inducing a shift into the spectral position of the reflection peak. Considering relatively small variations in temperature Δt and strain $\Delta \epsilon$ not to deviate from a linear behavior, the Bragg wavelength shift with respect to a reference temperature T_0 and strain ϵ_0 can be approximated as:

$$\Delta \lambda_{\mathrm{B}} = \lambda_{\mathrm{B}}(T_0, \epsilon_0) - \lambda_{\mathrm{B}}(T_0 + \Delta T, \epsilon_0 + \Delta \epsilon) = \left.\frac{\partial \lambda_{\mathrm{B}}}{\partial T}\right|_{\mathrm{T}_0} \Delta T + \left.\frac{\partial \lambda_{\mathrm{B}}}{\partial \epsilon}\right|_{\epsilon_0} \Delta \epsilon. \tag{3}$$

As evidenced by Eq. 3, FBG-based sensors, like all optical sensors, suffer from an intrinsic cross sensitivity between strain and temperature. This means that strain induces a Bragg wavelength shift that cannot be distinguished from the Bragg wavelength shift induced by the temperature difference. Therefore, to perform an accurate, artifact free thermal gradient measurement, the strain in the sensing regions must be kept constant in order to be accounted for by a simple constant offset that can be lately subtracted. In practice, avoiding strain artifacts is not easy, especially in applicators for tumor laser ablation monitoring that are designed to be inserted in the body and therefore suffer from the perturbations due both to the surgeon and the patient movements. Since in these conditions there is no guarantee that the strain can be kept constant, methods to decouple the strain and temperature contribution in the Bragg wavelength shift should be considered. For example, it is possible to decouple temperature and strain contributions by means of superstructure FBGs [28] or using an all fiber multi-parameter sensor based on sandwiching an FBG in a single mode fiber between two patches of multi mode fiber [29]. However, these approaches are hardly feasible when it comes to chains of closely spaced gratings (as those required for the targeted applications) because they require quite extended sensing regions to guarantee a large enough resolution. A more promising alternative is writing two FBGs with different sensitivity to strain and temperature per sensing point, resulting in a system of two equation that can then be easily inverted during the data post-processing [30, 31]. In particular, to have a different sensitivity to strain and temperature, the FBGs can be written

on the opposite sides of a splice between two fibers having the same core but different cladding diameters or, even better for the compactness, the two FBGs can be closely spaced along the same fiber but in correspondence of one of them the cladding is slightly reduced by chemical etching or mechanical polishing. In the end both approaches may be used to decouple the temperature and strain contribution from the Bragg wavelength shift but at the cost of increasing the complexity of the fabrication of dense FBGs chains.

The fully distributed temperature sensing has been investigated by measuring the Rayleigh scattering along a Single-Mode Fiber (SMF). Rayleigh scattering is due to stochastic inhomogeneities, small with respect to the wavelength and intrinsic in the fiber structure [32]. It is therefore evident that the amount of scattered light is influenced by local perturbations of the fiber structure.

In the experiments described in Sect. 3 the Rayleigh backscattering is measured by means of an Optical Backscatter Reflectometer (OBR 4600 by Luna Technologies®), which exploits Optical Frequency Domain Reflectometry (OFDR), which is a swept-wavelength interferometry to monitor the shift in the reflected spectrum induced by temperature or strain changes. More in detail, with reference to Fig. 2, the signal generated by a tunable laser that linearly sweeps the frequency over time is split by a coupler in two paths in an interferometric scheme: the first path constitutes the reference arm of the interferometer, while the second is the actual sensing arm. A mirror at the end of the reference arm and the Rayleigh backscattering in the measurement arm generate two reflected signals that are recombined at the coupler forming an interference pattern due to different path lengths caused by the distributed backscattering events in the sensing fiber. Then, through a Fourier Transform the beat frequencies are extracted, shown as peaks, and by using a linearly swept optical frequency they are brought back to the backscattering event as a function of fibre length.
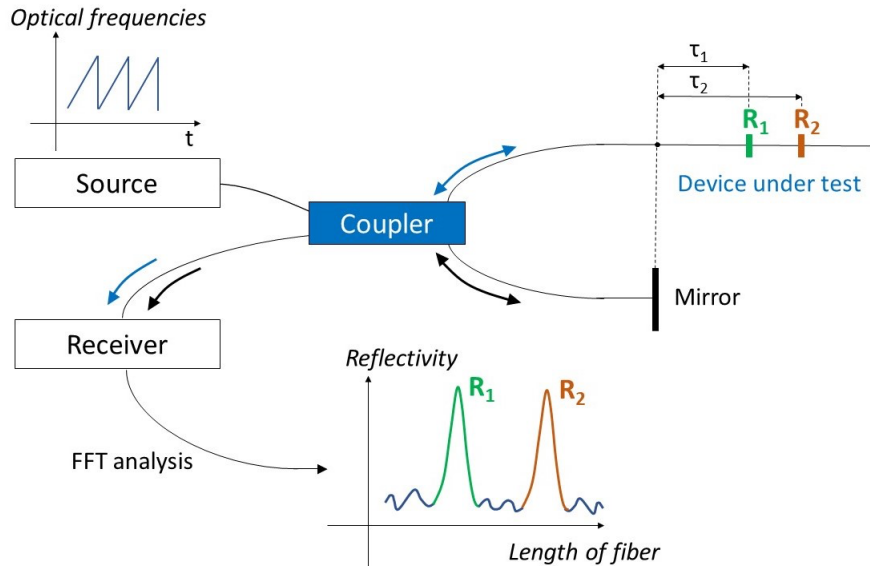

Figure 2: Scheme of the working principle of the OFDR instrument.

The instrument can have a sampling resolution of $10\,\mu m$ over tens of meters long fiber, with

a measurement rate ranging from about $0.8\,\mathrm{Hz}$ to $0.07\,\mathrm{Hz}$ (corresponding to scan times varying from $1.3\,\mathrm{s}$ to $15\,\mathrm{s}$) depending on the combination of the settings.

From the above considerations it is evident that for biomedical applications like LA in which the temperature can increase quite rapidly in some localized points, a setup capable of a fast response such as a quasi-distributed temperature measurement system based on multiplexed FBGs would be preferable (of course, provided that a custom sequence of gratings with suitable spacing is available); on the other hand, for the same application, the large temperature gradients would require a truly distributed sensing system. It should also be considered that the two interrogating instruments have much different costs, with the distributed one being way more expensive. However, the distributed system makes use of standard SMF, whereas the quasi-distributed requires a very expensive and complex setup to write customized fiber gratings with suitable Bragg wavelength and position along the sensing fiber. Besides for these considerations, it is important to evaluate the performance of these two approaches from the measurement point of view; this is described in Sect. 3.

3   Experiments

The comparison between the above described distributed and quasi-distributed temperature sensors has been carried out by means of three sets of experiments: one making use of a climatic chamber to generate a uniform temperature along the whole fibers, another using an *ad-hoc* setup devised to generate a linear thermal gradient, and the third one during an ex-vivo LA of a bovine liver.

3.1   Manufacturing of the FBG array : experimental setup and results
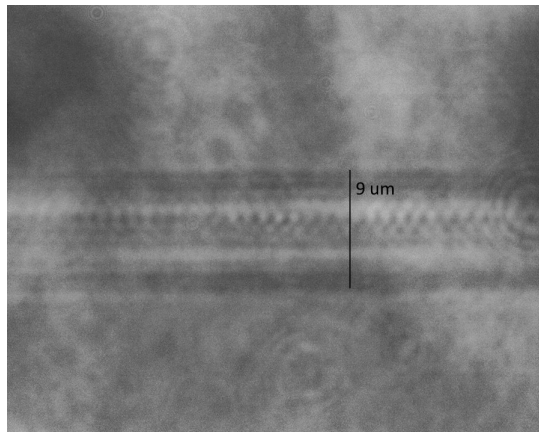

Figure 3: Point by point inscribed FBGs as seen from the femtosecond writing setup machine vision system.

The FBGs have been manufactured by direct writing through the coating using a $515\,\mathrm{nm}$ femtosecond laser using a point by point technique [33] because this technique is fast, flexible and, considering the $\sim 9\,\mu\mathrm{m}$ core diameter, adequate to obtain a peak reflectivity suitable for

being easily detected by the sensor interrogator. Fig. 3 shows a picture of one of the written gratings as seen from the femtosecond machine vision system. As already mentioned, the direct writing approach allows the inscribing each grating independently from the others, so that each can have a different Bragg wavelength and therefore be an independent sensing point along the fibre. The key parameters in the design of the array of FBGs are the separation between two adjacent FBGs, ΔL, the length of each FBG, l_{FBG}, and the wavelength interval between two adjacent Bragg wavelengths, $\delta\lambda_B$. The measurement resolution is determined by the couple ΔL and l_{FBG}; the latter influences also the error due to a non uniform temperature along the grating [22–24], while $\delta\lambda_B$ impacts the dynamic range. In particular:

- ΔL must be small enough to sample effectively the temperature gradient as it defines the spatial resolution of the FBG array assuming that l_{FBG} is negligible; clearly, in choosing this parameter also the total length of the region under measure and the maximum number of peaks that can be tracked by the interrogation software must be taken into account (but these are usually not a concern for LA applications and high performance FBG interrogators).

- l_{FBG} is determined as a compromise because on the one hand, a larger value increases the peak reflectivity and this improves the signal-to-noise ratio and thus the peak detection by the interrogation software; on the other hand, a smaller value allows considering negligible the temperature gradient along the grating.

- $\delta\lambda_B$ is determined as a compromise too, taking into account the maximum spectral bandwidth of the interrogator (100 nm for the instrument used in the reported experiments), the number of FBG multiplexed along the fiber (in turn defining the length of the sensing region with ΔL), their full width at half maximum, and the expected spectral shift from the temperature interval under measure.

For the experiments described in the following, an array of 15 FBGs with $\Delta L = 2\,\text{mm}$, $l_{FBG} = 1\,\text{mm}$, and $\delta\lambda_B = 6\,\text{nm}$ has been manufactured; the measured spectrum at room temperature is reported in Fig. 4. Prior to its usage, the grating array has been characterized by generating several temperature cycles with an environmental chamber in the $20\,^\circ\text{C}$ to $120\,^\circ\text{C}$ range and recording the corresponding Bragg wavelength shift for each grating.

3.2 Constant temperature: experimental setup and results

In the first experiment, the FBG array and a piece of SMF bare fiber acting as the distributed sensor have been simultaneously placed in a climatic chamber to compare their responses in a constant temperature case and evaluate their uniformity along the entire sensing region. To minimize strain fluctuations due to the forced air circulating in the climatic chamber, both sensors have been inserted in a thin glass capillary (i.e. $\sim 1\,\text{mm}$ external diameter, $10\,\text{cm}$ length) and then positioned on an aluminum bar using thermal grease.

The SMF fiber has been protruded for $29.7\,\text{cm}$ to take into account that the high reflectivity at the unconnected end of the fiber (although scissor cut and not cleaved) causes the Luna OBR
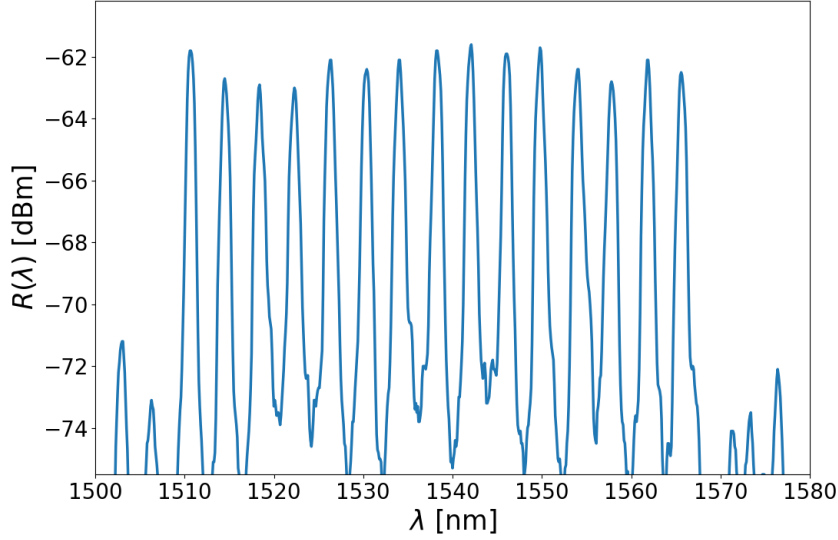
Figure 4: Reflection spectrum of the FBG array.

interrogator to be highly inaccurate in such last portion of the fiber, as shown in Fig. 5. Both quasi-distributed and fully distributed sensors extended beyond the region determined by the two external thermocouples.

Data from both the reference thermocouples and the FBGs have been acquired every 1 s. As for the Luna OBR, after proper calibration as described in the user's manual, it has been set with sensing range of 0.8 m, gauge length of 0.999 cm, and sensor spacing of 0.016 cm. The sensing range value has been chosen to highlight the portion of interest of the fiber.

The measurements have been taken at three temperature values ($\sim$ 20 °C, $\sim$ 35 °C and $\sim$ 50 °C) only after having reached a steady temperature condition. Both fiber sensors show an excellent uniformity, at the least for the target application, with small deviations in the actual portion of interest, which is the region delimited by the two external thermocouples. The 20 °C temperature has been used for setting the reference value of the Luna OBR and therefore the corresponding curve in Fig. 6 represents the residual error. The maximum error increases with temperature, from 0.2 °C and 0.9 °C at 35 °C for the FBGs and distributed sensor, respectively, to 2.04 °C and 1.5 °C at 50 °C, respectively. More details can be found in Fig. 6, Fig. 7, and Fig. 8 and in the corresponding Tab. 1, Tab. 2, and Tab. 3. In particular, Tab. 1, Tab. 2, and Tab. 3 report the average temperatures measured by the two sensors under test and the reference thermocouples along the portion of length 3 cm, corresponding to the length of the FBG-array.

It should be pointed out that the fiber sensors present an error with respect the thermocouples, which is due to an undesired local strain along the fibers and, as a minor effect, to the non-uniform temperature distribution within the climatic chamber. Indeed, the OFDR fiber and the FBG array have been inserted into the capillary by a certain force, thus generating an initial strain. In principle, such a strain could be compensated by referencing all following measurements; however, as the temperature changes, different thermal expansions of the capillary
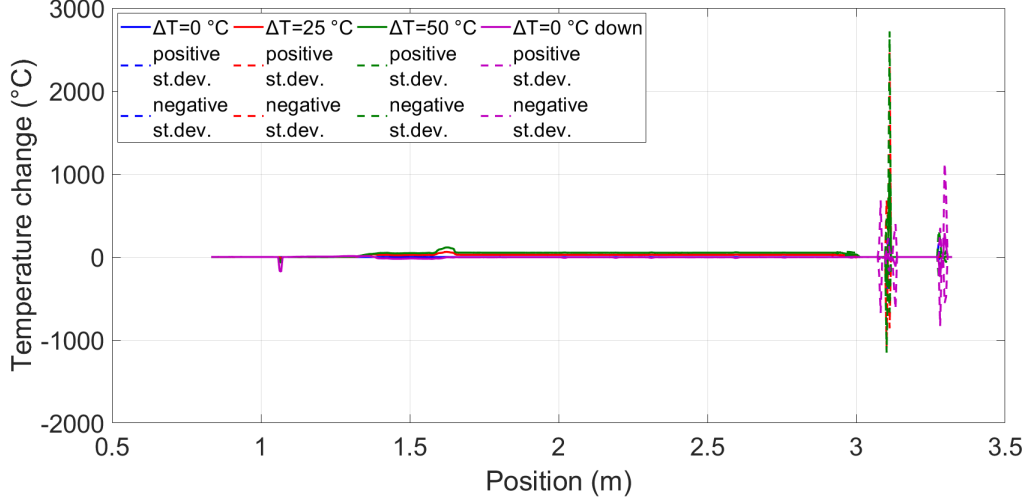
Figure 5: Example of distributed measurements (two traces overlapped) of a fiber kept at constant temperature demonstrating that the strong reflection from the unconnected fiber end makes the measurements in the last portion unreliable. The reported values are the temperature changes, considering that the starting temperature is 25 °C.

and the fibers, as well as the chamber vibrations, are likely to produce a change of the initial strain. This cannot be easily quantified, but its effect is well observable as a deviation from the expected flat temperature profile recorded by the thermocouples. These findings are depicted in Fig. 6, Fig. 7 and Fig. 8. In particular, with reference to Fig. 6, the OFDR plot is almost flat because its reference procedure has been performed at 20 °C when the fiber is already placed into the capillary. The temperature error with respect to the thermocouples is very small because the thermocouple readings have been employed as the reference value during the procedure and the effect of the fiber strain along the fiber has been thus cancelled. On the other hand, the FBG array shows a deviation because, having been already previously calibrated, no adjustment has been carried out during the test. Therefore, the array readings take into account both the actual temperature and the strain contributions. In Fig. 7 the readings from the FBG array and the OFDR show a small deviation from the expected constant temperature mainly due to the random strain introduced in both fibers by their contemporary presence in the capillary. The deviation in the area monitored by the reference thermocouples is less than 1 °C. Finally, the test at 50 °C in Fig. 8 shows a maximum error between the thermocouples and the fiber sensors of about 2 °C and an average error of 1.6 °C, highlighting an offset contribution that affects both fibers and that is compatible with an unwanted mechanical load. These deviations, although not playing a relevant role in hyperthermal applications – in those cases they are masked by much larger strains induced by the expansions and contractions of the tissue under ablation and by the involuntary movements of the patients [36] –, are nevertheless interesting from a metrological point of view and will be subject of further investigations.
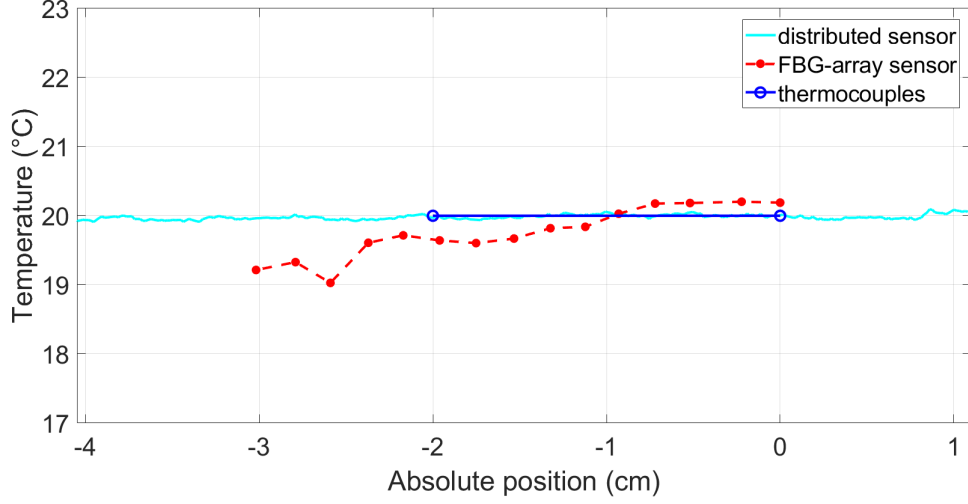
10

Figure 6: Comparison of the temperature readings using a climatic chamber to have a constant temperature; case of 20 °C. The cyan solid line is for the distributed sensor; the red dots are the readings of the gratings; the two blue circles the reading from the external thermocouples and the blue solid line the corresponding linear fitting.

Table 1: Mean temperatures of the curves in Fig. 6 along the 3 cm length of the FBG-array.

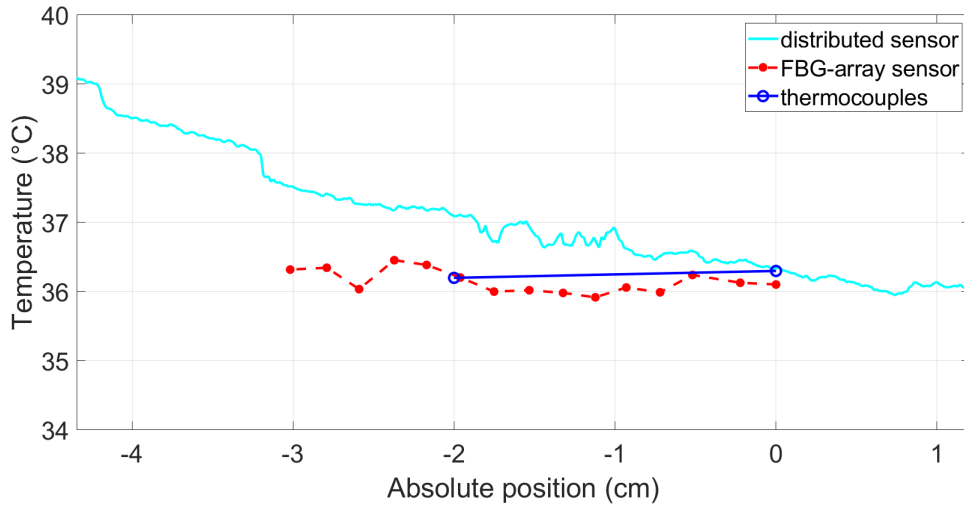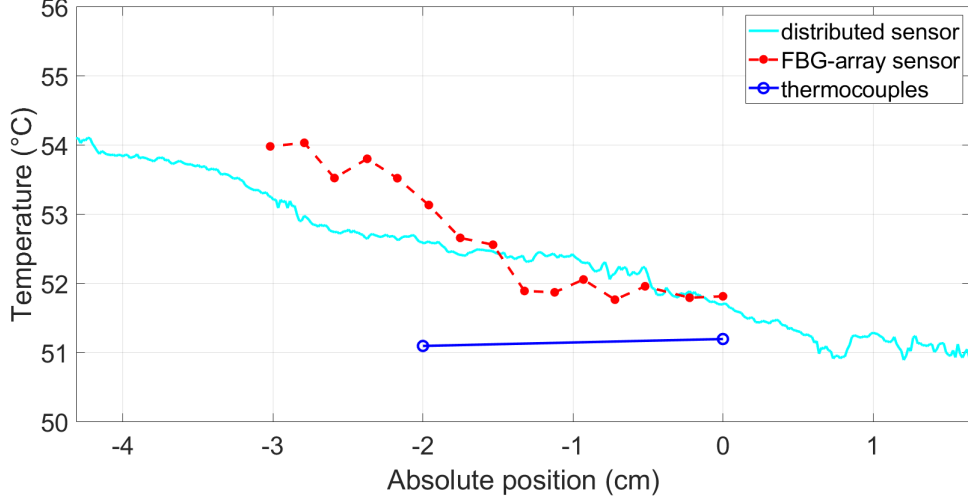|	T_{mean}
15-FBGs-array	19.75 °C
Distributed sensor	19.99 °C
Thermocouples	20 °C

Figure 7: Comparison of the temperature readings using a climatic chamber to have a constant temperature; case of ~ 35 °C. The cyan solid line is for the distributed sensor; the red dots are the readings of the gratings; the two blue circles the reading from the external thermocouples and the blue solid line the corresponding linear fitting.

Table 2: Mean temperatures of the curves in Fig. 7 along the 3 cm length of the FBG-array.

	T_{mean} (°C)
15-FBGs-array	36.15 °C
Distributed sensor	36.88 °C
Thermocouples	36.25 °C

Figure 8: Comparison of the temperature readings using a climatic chamber to have a constant temperature; case of ~ 50 °C. The cyan solid line is for the distributed sensor; the red dots are the readings of the gratings; the two blue circles the reading from the external thermocouples and the blue solid line the corresponding linear fitting.

Table 3: Mean temperatures of the curves in Fig. 8 along the 3 cm length of the FBG-array.

	T_{mean} (°C)
15-FBGs-array	52.70 °C
Distributed sensor	52.43 °C
Thermocouples	51.15 °C

3.3 The linear thermal gradient: experimental setup and results

The aim of the second experiment is the evaluation of the capability of both sensors to reconstruct a given temperature distribution. Therefore, a linear thermal gradient setup has been assembled to perform the experiment. The linear thermal gradient consist of a 2 mm thick aluminum bar shaped to have two much larger areas at the extremities that act as hot and cool sides hosting a heating resistor and a high thermal inertia block, respectively (Fig. 9).

According to Fourier's law of heat conduction, this configuration allows obtaining a linear temperature change in the central portion of the bar. The central area is 4 cm × 1 cm and has been milled to fabricate a groove to host the optical fiber sensors; a 4.9 cm × 6.2 cm × 4 cm
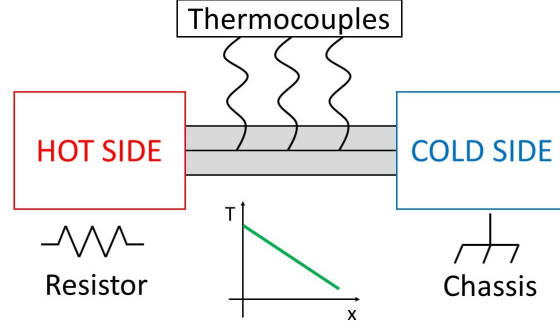
Figure 9: Schematic representation of the linear temperature gradient generator. Three thermocouples at equidistant positions are used as reference temperature sensors.

polystyrene block is positioned under the metal bar for thermal isolation. The hot side is heated by Joule effect through a $4\,\Omega$ resistor fixed under the metal, while the cold side is fixed to a large solid metal breadboard. Three T-type exposed-junction thermocouples to be used as temperature references are inserted in $1\,\mathrm{cm}$ spaced small holes drilled from the side of the metallic bar. The sensors under test are placed along the central portion of the bar, covered with thermal grease and further shielded with another polystyrene block to reduce temperature changes due to air convection. Fig. 10 shows the home made realization of this setup.
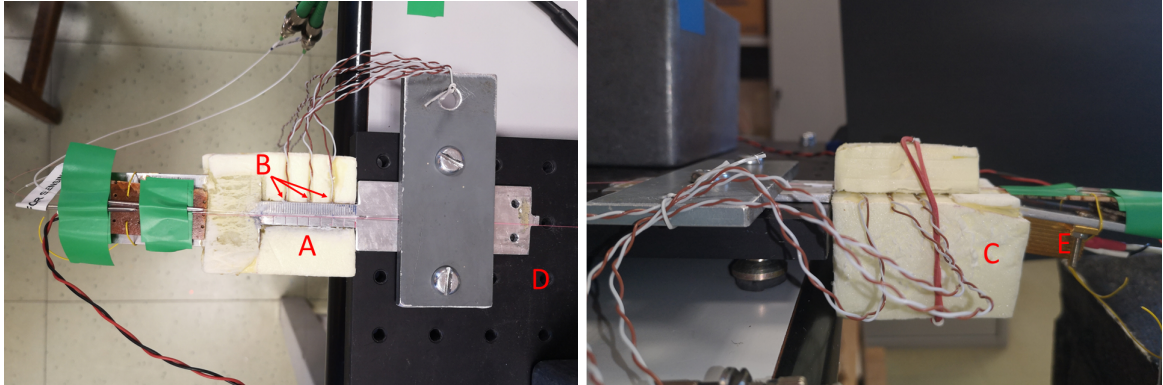

Figure 10: Photos of the home made setup to generate a linear temperature gradient: top (left) and left side (right) views. The central section A in which the linear gradient is generated, thermocouples B, the polystyrene block C, the large metal breadboard at the cold side D, and the resistor at the hot side E.

This setup has then been used to compare the behavior of a quasi-distributed temperature sensor made by an array of 15 multiplexed FBGs written with a femtosecond laser in a G.652-compliant single-mode optical fiber [34] and of fully distributed temperature sensor made by a unmodified piece of such fiber. In this case, since test has been performed outside the climatic chamber and thus without forced air, the capillary has not deemed to be necessary to shield the fibers and both sensors have been inserted in the bar groove as they were, coated with the thermal grease and further covered with the smaller polystyrene block. Again, the SMF fiber

has been protruded to avoid the perturbation effects due to the reflections from the fiber end facet.

The instrument parameters for both the MicronOptics FBG interrogator and the Luna OBR are the same as those used in the first experiment. The setup has been let to stabilize for ten minutes, reaching a stable thermal gradient corresponding to a difference of temperature between the two thermocouples at the extremes of the bar of $11.04\,°C$; then the temperature profile has been maintained for about 5 minutes. The comparison among the measured profiles is reported in Fig. 11. The measurements of both fiber sensors have the same slope of the reference line obtained from the temperatures measured by the thermocouples, even if there is a small offset error, especially for measurement obtained by the distributed system. This could be due to a parasitic strain induced while placing the fibers because the small fluctuations of the signal indicate that the distributed measures are very accurate. The gradient measured by the three sensors are detailed in Tab. 4.

Considering that for hyperthermal applications it is more important the temperature variation along the fiber rather than the initial absolute value, the errors (below $0.5\,°C$ for the gratings and below $2.5\,°C$ for the distributed system) are well acceptable for practical usages. Nevertheless, these results also show that the cross sensitivity with strain parasitic effects cannot be neglected for very high accuracy absolute temperature measurements.
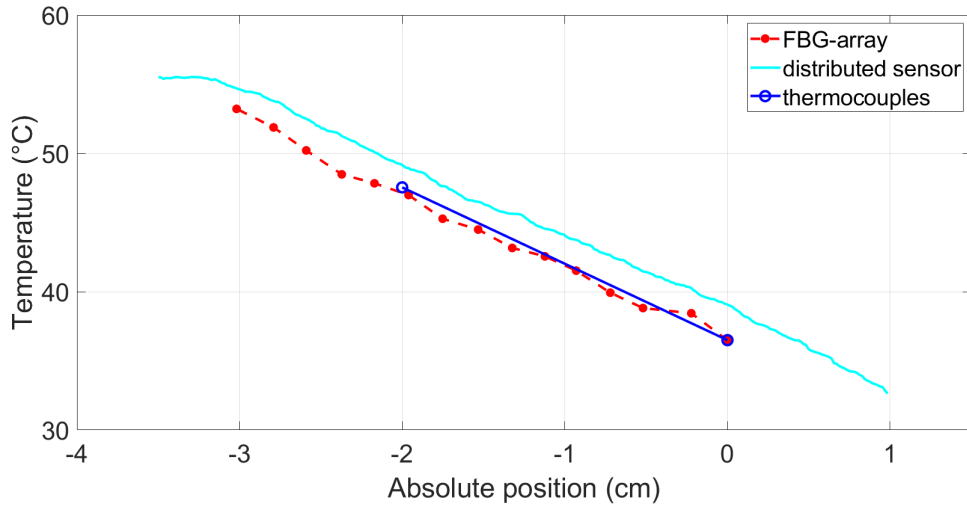

Figure 11: Comparison of the temperature readings using the linear gradient setup. The cyan solid line is for the distributed sensor; the red dots are the readings of the gratings; the two blue stars the reading from the external thermocouples and the blue dashed line the corresponding linear fitting. The origin is placed at the end of the FBG array, while the fully distributed sensor protrudes beyond the most distal FBG of the array inscribed.

Table 4: Temperature gradients computed from the data shown in Fig. 11.

	Gradient (°C/mm)
15-FBGs-array	0.54 °C/mm
Distributed sensor	0.52 °C/mm
Thermocouples	0.55 °C/mm

3.4 Ex-vivo experiments

The previous experimental comparison have showed promising results for the use of both the quasi-distributed and distributed fiber sensors, but they have been conducted with specific setups and in controlled environment. Therefore, to better assess their performance in a more operative condition, the third experiment has been the simulation of a laser ablation procedure monitoring using an *ex-vivo* bovine liver.

For this experiment a 200 µm core fiber, acting as the applicator, has been sandwiched in between two slices of liver and used to deliver a light beam from a high power laser diode module emitting at 915 nm [6, 35]. The 15 FBG array and the standard SMF used as distributed sensor have been positioned, one next to the other, in a direction perpendicular to the applicator fiber having its tip roughly in the middle of the sensing region of both fibers (clearly, the exact positioning is mainly relevant for the grating array), as sketched in Fig. 12.
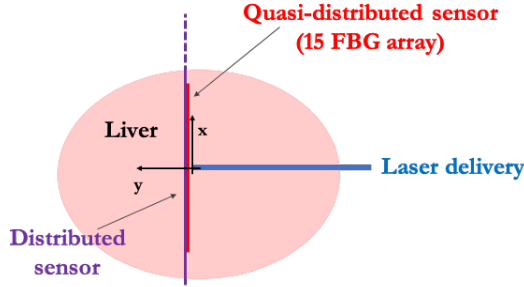

Figure 12: Sketch of the positioning of the distributed and quasi-distributed sensors for the ex-vivo experiment.

Since the goal of the experiment was a comparison of the two sensors and not an actual ablation procedure, the laser power has been arbitrary set to 2 W, for a duration of ∼ 3 min. Since the quasi-distributed sensing system, which has an acquisition rate of 1 kHz and whose data have been saved with a frequency of 1 Hz, supports a faster acquisition rate than the distributed system, 4 readings can be acquired in the time frame corresponding to the distributed sensor acquisition rate. The temperature profiles obtained from both sensors are very similar. As an example, here two cases are considered: one at 2 min and 47 s (Fig. 13), which is slightly before interruption of the laser irradiation, and another at 3 min and 15 s (Fig. 14), which is slightly after the irradiation interruption. As can be seen in Fig. 13, while the delivery fiber is still irradiating power into the liver tissue, the peak of the quasi-distributed sensor shows a slightly

higher temperature value due to the different distance of the two sensors from the fiber tip (which, although small, is relevant due to the large temperature gradients). Indeed, the quasi distributed sensor is practically in contact with the applicator fiber tip, while the distributed sensor is 1 mm away from it, so there is a relative distance between the two sensors of 1 mm. However, once the laser irradiation is stopped a steady state as been achieved, the two sensors reach an almost ideal agreement, practically overlapping, as shown in Fig. 14.
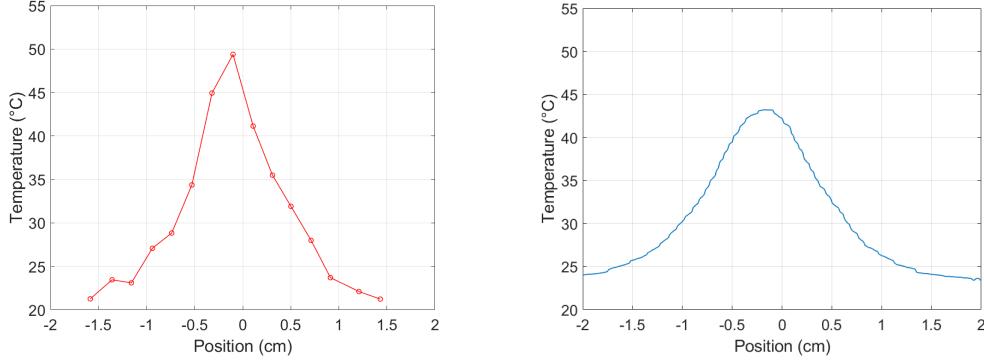

Figure 13: Comparison of the temperature readings around 2 min and 47 s: quasi-distributed sensor (left) and distributed sensor (right).
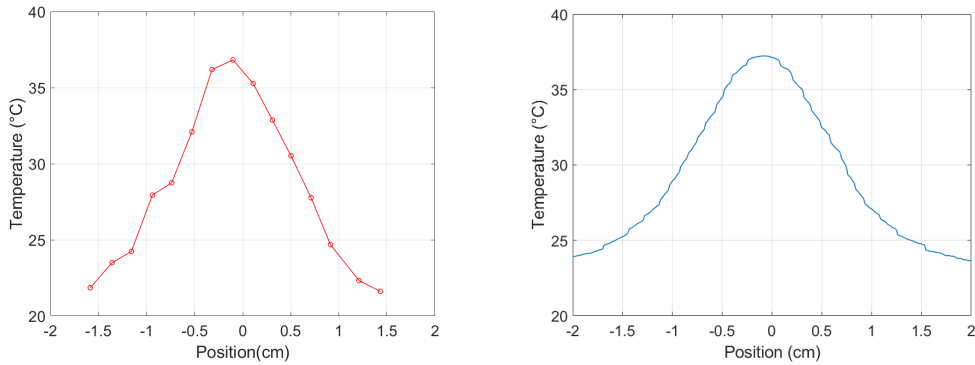

Figure 14: Comparison of the temperature readings around 3 min and 15 s: quasi-distributed sensor (left) and distributed sensor (right).

4   Discussion and conclusions

In this paper a quasi-distributed and a distributed fiber optic sensing systems devised to monitor the temperature distribution during hyperthermal tumor ablation treatments have been analyzed and their behavior compared with three experiments.

The quasi-distributed sensing system is based on a dense array of 15 fiber Bragg gratings written in a single fiber span with a femtosecond laser through a point by point procedure. This fabrication technique allows the fabrication of customized and highly dense grating arrays, with

a few millimeter spacing among them and therefore temperature measurement with a very high spatial resolution. Indeed, fifteen gratings, each 1 mm long and with 2 mm spacing, have been written for the array employed in the reported experiments. Moreover the high acquisition rate of the quasi-distributed system allows monitoring even the most rapid temperature variations that can occur during tumor laser ablations.

On the other hand, the analysis of the distributed sensing has been made exploiting the sensitivity of the Rayleigh scattering signature in standard single-mode fiber with the local temperature and strain variation. All the experiments pointed out the great potentiality of the optical frequency domain reflectometry employed in the interrogation instrument. This technology allows performing measurements that combine a temperature resolution similar to that achievable with the quasi-distributed approach (i.e., down to 0.1 °C), but with an unrivaled spatial resolution, which can be well below the millimeter and therefore practically unachievable in the quasi-distributed sensing. Moreover, this technique is not limited to very short lengths if a high spatial resolution is required, as it permits measuring temperature and the strain variations with sub-millimeter resolution along a several meter long fiber (i.e., at least 30 m with base instrument configuration). However, this technology is much more expensive than the interrogators employed for sensing with the FBGs, although costs can be somehow balanced in routine measurements with disposable probes (as it is customary in biomedical applications) considering that it uses a piece of standard single-mode fiber, while the quasi-distributed approach requires the inscription of an hoc array of dense gratings. Other drawbacks of the distributed sensing system are the longer time taken for a single measurement that limits its application when monitoring transient cases and the impossibility to measure close to the fiber end due to the perturbations originated by the reflection at the fiber end that prevails on the small Rayleigh scattering contribution.

Finally, the comparison between the quasi-distributed and the distributed sensing systems highlights that in all the experiments described in this paper the most critical aspect for both is the cross-sensitivity between temperature and strain phenomena. Indeed strains lead to an offset temperature error that cannot be compensated or corrected because often unpredictable and not constant. This issue is particularly critical in performing temperature measurements during *in-vivo* tumor laser ablation, where the insertion of the fiber and the cardiac or breathing motion artifacts could induce relevant errors. A first solution is to embody the sensors in protective capillaries but their optimization in order to improve the strain rejection while not affecting too much the temperature sensitivity and the invasive impact need further investigations in future experiments.

References

[1] E. Udd, W.B. Spillman Jr., Fiber optic sensors: an introduction for engineers and scientists, second ed., John Wiley & Sons, 2011.

[2] V. Budinski, D. Donlagic, 2017. Fiber-optic sensors for measurements of torsion, twist and rotation: a review. Sensors 17, 443.

[3] D. Tosi, G. Perrone, Fiber-optic sensors for biomedical applications, Artech House, 2017.

[4] D. Tosi, S. Poeggel, I. Iordachita, E. Schena, Fiber optic sensors for biomedical applications, in: H. Alemohammad (Ed.), Opto-Mechanical Fiber Optic Sensors, Butterworth-Heinemann, 2018, pp. 301–333.

[5] Y.J. Rao, D.J. Webb, D.A. Jackson, L. Zhang, I. Bennion, Optical in-fiber Bragg grating sensor systems for medical applications, J. Biomedical Optics 3 (1998) 38–44.

[6] R. Gassino, Y. Liu, A. Vallan, M. Konstantaki, S. Pissadakis, G. Perrone, A fiber optic probe for tumor laser ablation with integrated temperature measurement capability', J. Lightwave Technol. 35 (2017), 3447–3454.

[7] Distributed fiber optic sensing market. . .- Global Forecast to 2022, MarketsandMarket, 2016.

[8] Distributed fiber optic sensor market. . .Forecasts, 2019 – 2025, Grand View Research, 2019.

[9] X. Bao, L. Chen, Recent progress in distributed fiber optic sensors, Sensors 12 (2012), 8601–8639.

[10] D. Tosi, E. Schena, C. Molardi, S. Korganbayev, Fiber optic sensors for sub-centimeter spatially resolved measurements: Review and biomedical applications, Optical Fiber Technology 43 (2018), 6–19.

[11] D. Holler, R. Vaghetto, Y. Hassan, 2019. High-resolution wall temperature measurements with distributed fiber optic sensors, Int. J. of Thermal Sciences 145, 106042.

[12] R. Gassino, A. Vallan, G. Perrone, M. Konstantaki, S. Pissadakis, Characterization of fiber optic distributed temperature sensors for tissue laser ablation, Proc. IEEE Int. Instrumentation and Measurement Technology Conference (I2MTC) (2017), pp. 5.

[13] P. Saccomandi, A. Varalda, R. Gassino, et al., Linearly chirped fiber Bragg grating response to thermal gradient: from bench tests to the real-time assessment during in vivo laser ablations of biological tissue, J. of Biomedical Optics 22 (2017), 9.

[14] S. Korganbayev, Y. Orazayev, S. Sovetov, et al., Detection of thermal gradients through fiber-optic Chirped Fiber Bragg Grating (CFBG): medical thermal ablation scenario, Optical Fiber Technology 41 (2018), 48–55.

[15] S. Sartori, F. Di Vece, F. Ermili, P. Tombesi, Laser ablation of liver tumors: An ancillary technique, or an alternative to radiofrequency and microwave?, World J. Radiol. 9 (2017), 91–96.

[16] E. Schena, P. Saccomandi, D. Tosi, et al., Solutions to improve the outcomes of thermal treatments in oncology: multipoint temperature monitoring, IEEE J. of Electromagnetics, RF and Microwaves in Medicine and Biology 2 (2018), 172–178.

[17] M.G. Tanner, S.D. Dyer, B. Baek, R.H. Hadfield, S. Woo Nam, 2011. High-resolution single-mode fiber-optic distributed Raman sensor for absolute temperature measurement using superconducting nanowire single-photon detectors, Appl. Phys. Lett. 99, 201110.

[18] Y. Mizuno, N. Hayashi, H. Fukuda, K.Y. Song, K. Nakamura, 2016. Ultrahigh-speed distributed Brillouin reflectometry, Light Sci. Appl. 5, e16184.

[19] D.K. Gifford, B.J. Soller, M.S. Wolfe, M.E. Froggatt, Distributed fiber-optic temperature sensing using Rayleigh backscatter, 31st European Conference on Optical Communication, ECOC 2005 (2005).

[20] J. Bos, J. Klein, M.E. Froggatt, E. Sanborn, D. K. Gifford, 2013. Fiber optic strain, temperature and shape sensing via OFDR for ground, air and space applications, SPIE Proc. 8876, 887614.

[21] D. Tosi, 2017. Review and analysis of peak tracking techniques for fiber Bragg grating sensors, Sensors 17, 2368.

[22] R. Gassino, G. Perrone, A. Vallan, Temperature monitoring with fiber Bragg grating Sensors in non-uniform conditions, IEEE Trans. Instrum. Meas. 69 (2019), 1336–1343.

[23] R. Gassino, A. Vallan, G. Perrone, Evaluation of temperature measurement errors due to FBG sensors during laser ablation of ex-vivo porcine liver, Proc. IEEE Int. Instrumentation and Measurement Technology Conference (I2MTC) (2018).

[24] R. Gassino, J. Pogliano, G. Perrone, A. Vallan, Issues and characterization of fiber Bragg grating based temperature sensors in the presence of thermal gradients, Measurement 124 (2018), 15–19.

[25] S.J. Mihailov, C.W. Smelser, P. Lu, R.B. Walker, D. Grobnic, H. Ding, J. Unruh, Fiber Bragg gratings (FBG) made with a phase mask and 800 nm femtosecond radiation, OFC 2003 Optical Fiber Communications Conference (2003).

[26] S.J. Mihailov, D. Grobnic, C. Hnatovsky, R.B. Walker, P. Lu, D. Coulas, H. Ding, Extreme environment sensing using femtosecond laser-inscribed fiber Bragg gratings, Sensors 17 (2017).

[27] T. Erdogan, Fiber grating spectra, J. Lightwave Technol. 15 (1997), 1277–1294.

[28] H. Alemohammad, Superstructure fiber Bragg grating sensors for multiparameter sensing, Opto-Mechanical Fiber Optic Sensors, in Research, Technology, and Applications in Mechanical Sensing, Butterworth-Heinemann (2018), 27–47.

[29] D.P. Zhou, L. Wei, W.K. Liu, J.W.Y. Lit, Simultaneous strain and temperature measurement with fiber Bragg grating and multimode fibers using an intensity-based interrogation method, IEEE Phot. Technol. Lett. 21 (2009), 468–470.

[30] B. Hopf, F.J. Dutz, T. Bosselmann, M.Willisch, A.W. Kock, J. Roths, Iterative matrix algorithm for high precision temperature and force decoupling in multi-parameter FBG sensing, Optics Express 26 (2018), 12092–12105.

[31] M.C. Wu, R.H. Pater, S.L. DeHaven, Effects of coating and diametric load on fiber Bragg gratings as cryogenic temperature sensors, Proc. SPIE 6933 (2008).

[32] M. Nakazawa, Rayleigh backscattering theory for single-mode optical fibers, J. Opt. Soc. Am. 73 (1993), 1175–1180.

[33] W. Wang, J. Chen, Z. Liu, Point-by-point fiber gratings inscription by using high repetition rate femtosecond laser, 2019. SPIE Proc. 11333, 209–214.

[34] ITU-T Recommendation, G.652: Characteristics of a single-mode optical fibre and cable, 2016.

[35] R. Gassino, J. Pogliano, A. Vallan, D. Tosi, G. Perrone, Temperature distribution mapping using an FBG-equipped probe for solid tumor laser ablation, 13th IEEE International Symposium on Medical Measurements and Applications (MeMeA) (2018).

[36] P. Saccomandi, E. Schena, S. Silvestri, Techniques for temperature monitoring during laser-induced thermotherapy: an overview, Int. J. of Hyperthermia 29 (2013), 609–619.